Original paper

# Clinical and magnetic resonance imaging features predict microvascular invasion in intrahepatic cholangiocarcinoma

**Jin-Jun Sun[1], Xian-Ling Qian[2,3,4], Yi-Bing Shi[1], Yu-Fei Fu[1], Chun Yang[2,3,4], Xi-Juan Ma[1]**

[1]Department of Radiology, Xuzhou Central Hospital, Xuzhou Clinical School of Xuzhou Medical University, Xuzhou, China
[2]Department of Radiology, Zhongshan Hospital, Fudan University, Shanghai, China
[3]Shanghai Institute of Medical Imaging, Shanghai, China
[4]Department of Cancer Center, Zhongshan Hospital, Fudan University, Shanghai, China

Gastroenterology Rev 2023; 18 (2): 161–167
DOI: https://doi.org/10.5114/pg.2022.116668

**Key words:** intrahepatic cholangiocarcinoma, microvascular invasion, magnetic resonance imaging.

**Address for correspondence:** MD Xi-Juan Ma, Department of Radiology, Xuzhou Central Hospital, Xuzhou Clinical School of Xuzhou Medical University, Xuzhou, China, e-mail: xjma1234@163.com

## Abstract

**Introduction:** Clinical features and magnetic resonance imaging (MRI)-related data are commonly employed in clinical settings and can be used to predict the microvascular invasion (MVI) status of intrahepatic cholangiocarcinoma (ICC) patients.

**Aim:** To generate a clinical and MRI-based model capable of predicting the MVI status of ICC patients.

**Material and methods:** Consecutive ICC patients evaluated from June 2015 to December 2018 were retrospectively enrolled in a training group to establish a predictive clinical MRI model. Consecutive ICC patients evaluated from January 2019 to June 2019 were prospectively enrolled in a validation group to test the reliability of this model.

**Results:** In total, 143 patients were enrolled in the training group, of whom 46 (32.2%) and 96 (67.8%) were MVI-positive and MVI-negative, respectively. Logistics analyses revealed larger tumour size ($p = 0.008$) and intrahepatic duct dilatation ($p = 0.01$) to be predictive of MVI positivity, enabling the establishment of the following predictive model: $-2.468 + 0.024 \times$ tumour size $+ 1.094 \times$ intrahepatic duct dilatation. The area under the receiver operating characteristic (ROC) curve (AUC) for this model was 0.738 ($p < 0.001$). An optimal cut-off value of –1.0184 was selected to maximize sensitivity (71.7%) and specificity (61.9%). When the data from the validation group were incorporated into the predictive model, the AUC value was 0.716 ($p = 0.009$).

**Conclusions:** Both larger tumour size and intrahepatic duct dilatation were predictive of MVI positivity in patients diagnosed with ICC, and the predictive model developed based on these variables can offer quantitative guidance for assessing the risk of MVI.

## Introduction

Intrahepatic cholangiocarcinoma (ICC) is the second most common form of liver malignancy, accounting for 10–15% of cases [1–4]. While surgical resection remains the optimal treatment option for ICC patients with resectable disease, postoperative progression rates are suboptimal, and the 5-year overall survival and disease-free survival rates of affected patients are estimated to be 55% and 41.7%, respectively [5].

Several clinical factors have been linked to poorer ICC patient prognosis, including more advanced age, lymph node metastasis, cancer antigen 19-9 (CA19-9) levels, and microvascular invasion (MVI), with MVI being the most commonly identified risk factor in this oncogenic setting [5–7]. However, at present MVI is a histological finding that can only be detected through the postoperative evaluation of resected surgical specimens, enabling clinicians to make more appropriate treatment plans and patient management decisions [8]. The ability to preoperatively predict MVI status based on clinical and/or radiological findings would thus be of significant value. Several studies to date have employed radiomics-based nomograms as tools for predicting the MVI status of ICC or hepatocellular carcinoma (HCC) patients [3, 9]. However, radiomics approaches are primarily applied at the experimental level rather than in clinical settings. In contrast, clinical features and magnetic

resonance imaging (MRI)-related data are commonly employed in clinical settings and can be used to predict ICC and HCC patient MVI status [4, 10].

## Aim

The present study was developed to generate a predictive model capable of predicting MVI status in ICC patients based on clinical and MRI features.

## Material and methods

### Patient selection

Our institutional review board approved this retrospective diagnostic study, and the requirement for written informed consent was waived.

Between June 2015 and December 2018, consecutive ICC patients were retrospectively enrolled into a training group for the development of a predictive MRI-based clinical model. Between January 2019 and June 2019, consecutive ICC patients were prospectively enrolled into a validation group to assess the reliability of the developed model.

Patients eligible for inclusion were those with the following: (a) ICC tumours confirmed following surgical resection; (b) mass-like ICC tumours; (c) lesions ≥ 10 mm in size; and (d) MRI imaging and clinical analyses conducted within 30 days prior to surgical resection. Patients were excluded from this study if they exhibited: (a) multiple ICC tumours; (b) recurrent ICC after surgery; (c) had undergone preoperative antitumour treatment; (d) had incomplete clinical data; or (e) exhibited MRI images of poor quality.

### MRI analysis

The MRI scanning systems used to evaluate patients included in the present study included a 1.5-T UIHMR 560 scanner (Shanghai United Imaging Healthcare, China); a 3.0-T UIHMR 770 MR imager (Shanghai United Imaging Healthcare); a Magnetom Avanto 1.5-T imager (Siemens Healthcare, Germany); a Magnetom Aera 1.5 T imager (Siemens Healthcare); a Magnetom Verio 3.0-T MRI System (Siemens Healthcare); a GE750 (3.0-T MR system, Discovery MR 750, GE Healthcare); and a Philips Intera Achieva 1.5T MR System (Philips Medical Systems, Netherlands). Collected MRI image types included diffusion-weighted imaging (DWI), T1WI, T2WI, and Gd-DTPA-enhanced images. For further details regarding the utilized acquisition sequences (Table I).

Two radiologists, each with over 10 years of MRI experience, who were blinded to the patients' pathological and clinical findings, analysed all MRI scans. Any discrepancies between these reviewers were resolved by a third experienced radiologist with over 20 years of experience. All evaluated MRI features are compiled in Table II.

### Clinical data

Clinical data included in the present analyses were collected from patient medical records and included age, gender, history of hepatitis B viral infection, and levels of tumour markers including carcinoembryonic antigen (CEA), α-fetoprotein (AFP), and CA19-9 (Table II).

A team of experienced pathologists, each of whom had over 10 years of relevant experience interpreting histopathological sections, who were blinded to radiological and clinical results, conducted all pathological analyses of resected tumour sections.

### Definitions

MVI was defined by the presence of tumour cells within an endothelium-lined vascular region at the interface between the tumour periphery and the hepatic parenchymal tissue that was only detectable upon microscopic evaluation [4]. The presence of peripheral diffusion restriction with central isointensity/hypointensity was indicative of MRI target sign [3]. Tumour MRI intensity was determined with reference to the intensity of the normal liver parenchyma. Maximal tumour diameter was used to define tumour size [4]. Enhancement restricted to the lesion periphery in the arterial

**Table I.** Magnetic resonance imaging sequences and parameters

| Parameter | FS-T2WI | T1-weighted IP and OP Imaging | FS-T1WI | DWI |
|---|---|---|---|---|
| Repetition time [ms] | 2693 | 115.8 | 4.43 | 2807 |
| Echo time [ms] | 85.58 | 4.4 and 2.2 | 2.2 | 75.7 |
| Section thickness [mm] | 6 | 6 | 3 | 6 |
| Matrix size | 201 × 288 | 230 × 288 | 192 × 256 | 115 × 128 |
| Field of view [mm$^2$] | 380 × 360 | 380 × 290 | 400 × 280 | 380 × 300 |
| Gap [mm] | 20 | 20 | 0 | 20 |
| NEX | 1 | 1 | 1 | 4 |

*FS – fat-suppression, IP – in-phase, OP – opposed-phase, DWI – diffusion-weighted imaging.*

**Table II.** Baseline data of patients in the training group.

| Parameter | MVI positive (*n* = 46) | MVI negative (*n* = 97) | *P*-value |
|---|---|---|---|
| Clinical data: | | | |
| Age [years] | 62.1 | 61.1 | 0.564 |
| Gender (male/female) | 32/14 | 69/28 | 0.785 |
| Hepatitis B virus (yes/no) | 20/26 | 52/45 | 0.258 |
| AFP (≥ /< 20 ng/ml) | 7/39 | 9/88 | 0.293 |
| CEA (≥ /< 5 ng/ml) | 14/32 | 17/60 | 0.302 |
| CA199 (≥ /< 34 U/ml) | 23/23 | 40/57 | 0.324 |
| MR features: | | | |
| Size [mm] | 61.0 | 43.4 | 0.001 |
| Tumour morphology (round/irregular) | 10/36 | 36/61 | 0.066 |
| Intrahepatic duct dilatation (yes/no) | 27/19 | 25/72 | < 0.001 |
| Hepatic capsular retraction (yes/no) | 21/25 | 37/60 | 0.517 |
| Signal on T1W (low/isointensity/high) | 43/2/1 | 95/2/0 | 0.252 |
| Signal on T2W-FS (low/isointensity/high) | 0/0/46 | 0/5/92 | 0.280 |
| Signal on DWI (low/isointensity/high) | 0/0/46 | 0/0/96 | – |
| Target sign on T2W (yes/no) | 19/27 | 41/56 | 0.913 |
| Target sign on DWI (yes/no) | 20/26 | 44//53 | 0.833 |
| Arterial rim enhancement on arterial phase (yes/no) | 38/8 | 83/14 | 0.647 |
| Dynamic enhancement pattern (progressive/wash in- wash-out/others) | 36/4/6 | 74/14/9 | 0.534 |
| Visible vessel penetration (yes/no) | 30/16 | 49/48 | 0.099 |
| Peritumoral parenchymal enhancement (yes/no) | 25/21 | 56/41 | 0.703 |

*AFP – alpha fetoprotein, CEA – carcinoembryonic antigen, CA199 – Carbohydrate antigen 199, FS – fat suppression, DWI – diffusion-weighted imaging, MVI – microvascular invasion.*

phase was indicative of arterial rim enhancement [3]. When visual inspection of the collected images revealed the invasion of adjacent portal veins, hepatic veins, or hepatic arteries, this was indicative of vessel penetration [11]. Grossly hyperarterial contrast enhancement outside of the border of the tumour, becoming isointense with the hepatic parenchymal background during layer dynamic phases, irrespective of shape, was indicative of peritumoral parenchymal enhancement [11]. Three types of dynamic enhancement pattern were defined for the purposes of this study: (a) progressive patterns, in which lesions exhibit progressive enhancement with maximal intensity or range on delayed phase; (b) wash in-wash out patterns, in which intense contrast uptake is evident during the arterial phase, but the agent is then washed out in the portal or delayed phases; and (c) others [3].

### Statistical analysis

Continuous data were analysed via independent sample *t*-tests, while categorical data were analysed via Pearson $\chi^2$ tests or Fisher's exact test. Predictors of MVI were identified through univariate and multivariate logistic regression analyses of data from patients in the training group, with the results of these analyses being used to construct a model capable of predicting MVI status. Area under the curve (AUC) values for receiver operating characteristic (ROC) curves were used to evaluate this model, with an appropriate cut-off value being calculated. $P < 0.05$ was the threshold of significance, and all data analyses were conducted using SPSS® v.16.0 (SPSS Inc., IL, USA).

## Results

### Training group analyses and model construction

In total, the training group enrolled 143 patients, of whom 46 (32.2%) and 97 (67.8%) were, respectively, MVI positive and MVI negative (Figure 1). Clinical and MRI data for patients in these 2 MVI cohorts are compiled in Table II.

In univariate logistic analyses, larger tumour size, higher CEA levels, intrahepatic duct dilatation, and irregular tumour morphology were predictive of MVI pos-

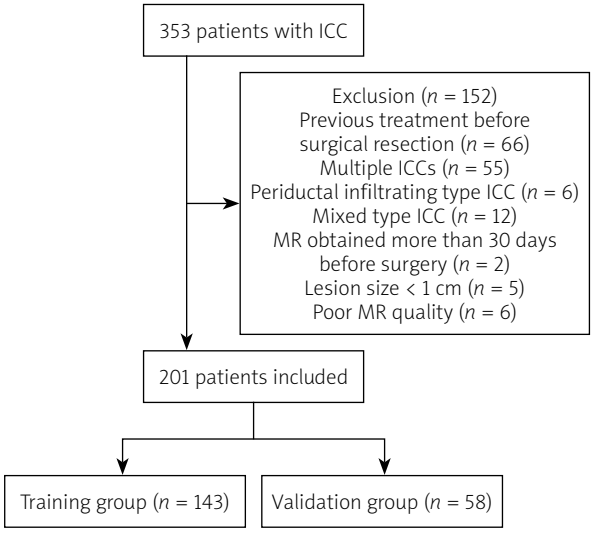


**Figure 1.** Flowchart of the study

itivity. When these 4 variables were incorporated into a multivariate logistic analysis, only larger tumour size (HR = 1.024; $p = 0.008$) and intrahepatic duct dilatation (HR = 2.985; $p = 0.01$) were confirmed to be predictive of MVI positivity (Table III).

A predictive model was next established based upon these variables as follows: –2.468 + 0.024 × size + 1.094 × intrahepatic duct dilatation (present = 1; absent = 0). The AUC of the ROC curve for this model was 0.738 (95% CI: 0.651–0.825, $p < 0.001$, Figure 2). A cut-off score of –1.0184 was selected to maximize sensitivity (71.7%) and specificity (61.9%), with values ≥ –1.0184 being predictive of MVI positivity, whereas values < –1.0184 were predictive of negative MVI status.

### Validation group

In total, 58 patients were enrolled in the validation cohort for this study (Table IV), of whom 18 (31.0%) and 40 (69.0%) patients were MVI positive and MVI negative, respectively. Similar rates of MVI positivity were observed when comparing the training and validation groups ($p = 0.876$). Most of the clinical and MRI data were comparable between these 2 patient cohorts (Table IV). When data from patients in the validation cohort were inserted into our predictive model, the AUC for the ROC curve was 0.716 (95% CI: 0.581–0.851, $p = 0.009$, Figure 3).

## Discussion

Here, we identified 2 risk factors associated with MVI positivity in ICC patients and used these factors to construct a predictive model. Both of these risk factors were MRI features, whereas no analysed tumour markers or clinical features were found to be associated with MVI status in the analysed patient cohort.

Multiple previous studies have found MVI to be indicative of poor prognostic outcomes in patients diagnosed with ICC, with adjuvant chemotherapy following R0 resection being the most appropriate treatment for MVI-positive patients [5, 12]. The ability to reliably gauge patient MVI status prior to surgical treatment is thus critical to improving patient outcomes.

We found tumour size to be a primary risk factor associated with MVI risk, with larger tumours being more likely to exhibit MVI positivity. This finding is consistent with previous data reported by Zhou *et al.* [13]. Similarly, Spolverato *et al.* [14] reported a 6-fold higher MVI incidence rate for tumours 3–5 cm in size as compared to tumours < 3 cm in size. We observed a significantly larger mean lesion size in MVI-positive patients relative to MVI-negative patients (61.0 mm vs. 43.4 mm, $p = 0.001$).

We additionally identified intrahepatic duct dilatation as a risk factor associated with MVI positivity. No prior studies have, to the best of our knowledge, examined the relationship between these 2 clinical findings. We observed a 2.3-fold higher MVI incidence rate for tumours exhibiting intrahepatic duct dilatation as compared to tumours without such dilatation. Intrahepatic duct invasion is the cause of intrahepatic duct dilatation [15], and it is thus rational that the ability of the tumour to infiltrate this duct is correlated with a higher risk of MVI.

**Table III.** Predictors of MVI positivity

| Variables | Univariate analysis | | | Multivariate analysis | | |
|---|---|---|---|---|---|---|
| | Hazard ratio | 95% CI | *P*-value | Hazard ratio | 95% CI | *P*-value |
| CEA | 2.059 | 0.909–4.663 | 0.083 | 1.336 | 0.524–3.405 | 0.544 |
| Size | 1.028 | 1.013–1.044 | < 0.001 | 1.024 | 1.006–1.042 | 0.008 |
| Tumour morphology: | | | | | | |
| Round | 1 | | | 1 | | |
| Irregular | 2.426 | 1.051–5.602 | 0.038 | 0.973 | 0.359–2.639 | 0.957 |
| Intrahepatic duct dilatation | 4.093 | 1.948–8.600 | < 0.001 | 2.985 | 1.294–6.886 | 0.01 |

*CEA – carcinoembryonic antigen, MVI – microvascular invasion.*

While higher levels of specific tumour markers, including CEA, CA19-9, and AFP, have been linked to reductions in overall and progression-free survival, they have largely not been found to be associated with ICC patient MVI status [7, 16–19]. Consistently, we observed no relationship between tumour marker levels and MVI positivity.

While we identified 2 risk factors that were independently associated with the risk of MVI positivity, in clinical practice their relative significance and associated clinical implications may not be immediately clear. As such, we developed a predictive model incorporating both of these risk factors in order to provide more quantitative guidance. The AUC for this model (0.738) was indicative of good predictive utility, and a similar AUC value in an independent 58-patient validation cohort (0.716) further confirmed the ability of this model to accurately predict patient MVI status.

There are certain limitations to the present analysis. Firstly, this was a retrospective study and thus subject to a high risk of selection bias. Secondly, we only analysed mass-like and resectable ICC tumours, whereas

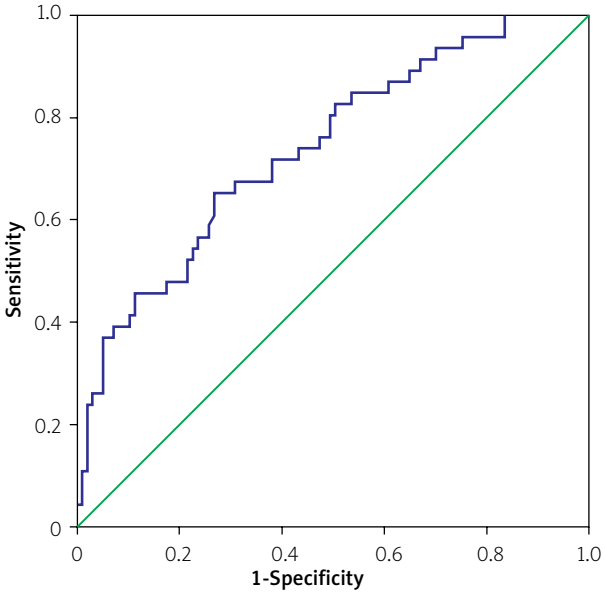


**Figure 2.** ROC curve generated using the predictor from the training group

**Table IV.** Baseline data of training and validation groups

| Parameter | Training group (*n* = 143) | Validation group (*n* = 58) | *P*-value |
|---|---|---|---|
| Clinical data: | | | |
| Age [years] | 61.4 | 60.3 | 0.166 |
| Gender (male/female) | 101/42 | 43/15 | 0.617 |
| Hepatitis B virus (yes/no) | 72/71 | 19/39 | 0.029 |
| AFP (≥ /< 20 ng/ml) | 16/127 | 10/48 | 0.247 |
| CEA (≥ /< 5 ng/ml) | 31/112 | 4/54 | 0.012 |
| CA199 (≥ /< 34 U/ml) | 63/80 | 22/36 | 0.426 |
| MVI (positive/negative) | 46/97 | 18/40 | 0.876 |
| MR features: | | | |
| Diameter [mm] | 49.1 | 43.7 | 0.552 |
| Tumour morphology (round/irregular) | 46/97 | 30/28 | 0.01 |
| Intrahepatic duct dilatation (yes/no) | 52/91 | 25/33 | 0.373 |
| Hepatic capsular retraction (yes/no) | 58/85 | 24/34 | 0.915 |
| Signal on T1W (low/isointensity/high) | 138/4/1 | 58/0/0 | 0.354 |
| Signal on T2W-FS (low/isointensity/high) | 0/5/138 | 0/1/57 | 1.000 |
| Signal on DWI (low/isointensity/high) | 0/0/143 | 0/0/58 | – |
| Target sign on T2W (yes/no) | 60/93 | 16/42 | 0.116 |
| Target sign on DWI (yes/no) | 64/89 | 28/30 | 0.399 |
| Arterial rim enhancement on arterial phase (yes/no) | 121/22 | 41/17 | 0.024 |
| Dynamic enhancement pattern (progressive/wash-in wash-out/others) | 110/18/15 | 39/8/11 | 0.239 |
| Visible vessel penetration (yes/no) | 79/64 | 35/23 | 0.508 |
| Peritumoral parenchymal enhancement (yes/no) | 81/62 | 32/26 | 0.649 |

*AFP – α-fetoprotein, CEA – carcinoembryonic antigen, CA199 – carbohydrate antigen 199, FS – fat-suppression, DWI – diffusion-weighted imaging, MVI – microvascular invasion.*

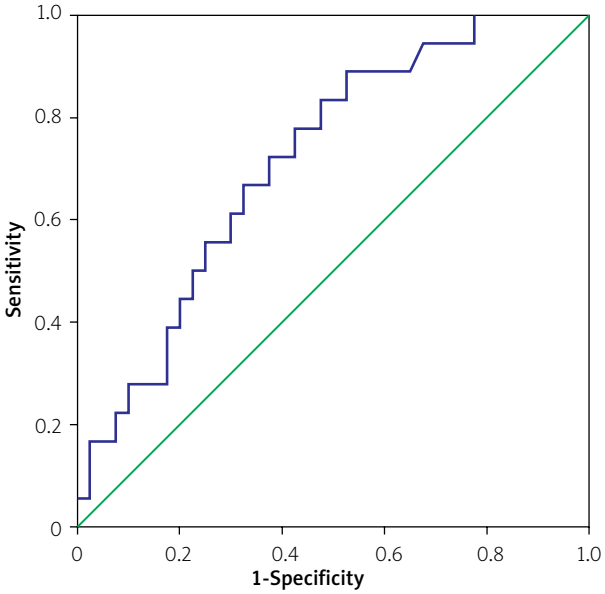


**Figure 3.** ROC curve generated using data from the validation group

inoperable ICCs and other pathological tumour types such as periductal-infiltrating, intraductal growing, and mixed-type ICCs were omitted, even though they may be more likely to develop MVI. As such, this model is only suitable for predicting MVI status in a specific subset of patients. Thirdly, only specific qualitative MRI features including DWI, T1W, T2W, and morphological features were incorporated into these analyses, whereas ADC values and quantitative MRI features were not assessed. Future studies incorporating these quantitative features are thus warranted. Lastly, while we conducted the prospective validation of our model in a distinct patient cohort, there were certain baseline values that differed significantly between the training and validation groups, thus potentially affecting the resultant data.

## Conclusions

Larger tumour size and intrahepatic duct dilatation are both predictive of MVI positivity in patients diagnosed with ICC. The predictive model incorporating these 2 variables can thus offer quantitative insights when predicting MVI status in the context of patient treatment and monitoring.

## Acknowledgments

This work is supported by The Development Research Foundation of Affiliated Hospital of Xuzhou Medical University (grant number: XYFM2020020) and The Medical Scientific Research Program of Jiangsu Commission of Health (grant number: M2021014).

## Conflict of interest

The authors declare no conflict of interest.

### References

1. Bergquist A, von Seth E. Epidemiology of cholangiocarcinoma. Best Pract Res Clin Gastroenterol 2015; 29: 221-32.
2. Sempoux C, Jibara G, Ward SC, et al. Intrahepatic cholangiocarcinoma: new insights in pathology. Semin Liver Dis 2011; 31: 49-60.
3. Zhou Y, Zhou G, Zhang J, et al. Radiomics signature on dynamic contrast-enhanced MR images: a potential imaging biomarker for prediction of microvascular invasion in mass-forming intrahepatic cholangiocarcinoma. Eur Radiol 2021; 31: 6846-55.
4. Ma X, Liu L, Fang J, et al. MRI features predict microvascular invasion in intrahepatic cholangiocarcinoma. Cancer Imaging 2020; 20: 40.
5. Tsukamoto M, Yamashita YI, Imai K, et al. Predictors of cure of intrahepatic cholangiocarcinoma after hepatic resection. Anticancer Res 2017; 37: 6971-5.
6. Cho SY, Park SJ, Kim SH, et al. Survival analysis of intrahepatic cholangiocarcinoma after resection. Ann Surg Oncol 2010; 17: 1823-30.
7. Tang Z, Liu WR, Zhou PY, et al. Prognostic value and predication model of microvascular invasion in patients with intrahepatic cholangiocarcinoma. J Cancer 2019; 10: 5575-84.
8. Shao C, Chen J, Chen J, et al. Histological classification of microvascular invasion to predict prognosis in intrahepatic cholangiocarcinoma. Int J Clin Exp Pathol 2017; 10: 7674-81.
9. Yang L, Gu D, Wei J, et al. A radiomics nomogram for preoperative prediction of microvascular invasion in hepatocellular carcinoma. Liver Cancer 2019; 8: 373-86.
10. Wang X, Wang W, Ma X, et al. Combined hepatocellular-cholangiocarcinoma: which preoperative clinical data and conventional MRI characteristics have value for the prediction of microvascular invasion and clinical significance? Eur Radiol 2020; 30: 5337-47.
11. An C, Kim DW, Park YN, et al. Single hepatocellular carcinoma: preoperative mr imaging to predict early recurrence after curative resection. Radiology 2015; 276: 433-43.
12. Ali SM, Clark CJ, Mounajjed T, et al. Model to predict survival after surgical resection of intrahepatic cholangiocarcinoma: the Mayo Clinic experience. HPB 2015; 17: 244-50.
13. Zhou Y, Wang X, Xu C, et al. Mass-forming intrahepatic cholangiocarcinoma: can diffusion-weighted imaging predict microvascular invasion? J Magn Reson Imaging 2019; 50: 315-24.
14. Spolverato G, Ejaz A, Kim Y, et al. Tumor size predicts vascular invasion and histologic grade among patients undergoing resection of intrahepatic cholangiocarcinoma. J Gastrointest Surg 2014; 18: 1284-91.
15. Kondo Y, Shiina S, Tateishi R, et al. Intrahepatic bile duct dilatation after percutaneous radiofrequency ablation for hepatocellular carcinoma: impact on patient's prognosis. Liver Int 2011; 31: 197-205.
16. Zheng BH, Yang LX, Sun QM, et al. A new preoperative prognostic system combining CRP and CA199 for patients with intrahepatic cholangiocarcinoma. Clin Transl Gastroenterol 2017; 8: e118.

17. Saito H, Noji T, Okamura K, et al. A new prognostic scoring system using factors available preoperatively to predict survival after operative resection of perihilar cholangiocarcinoma. Surgery 2016; 159: 842-851.
18. Li H, Feng Y, Liu C, et al. Importance of normalization of carbohydrate antigen 19-9 in patients with intrahepatic cholangiocarcinoma. Front Oncol 2021; 11: 780455.
19. Qiu H, Liu C, Huang M, et al. Prognostic value of combined CA19-9 with aspartate aminotransferase to lymphocyte ratio in patients with intrahepatic cholangiocarcinoma after hepatectomy. Cancer Manag Res 2021; 13: 5969-80.

**Received:** 8.03.2022
**Accepted:** 28.03.2022